SIMULATION OF CASCADED LONGITUDINAL-SPACE-CHARGE AMPLIFIER AT THE FERMILAB ACCELERATOR SCIENCE & TECHNOLOGY (FAST) FACILITY*

A. Halavanau[1], and P. Piot[1,2]
[1] Department of Physics and Northern Illinois Center for Accelerator & Detector Development, Northern Illinois University, DeKalb, IL 60115, USA
[2] Accelerator Physics Center, Fermi National Accelerator Laboratory, Batavia, IL 60510, USA

Abstract

Cascaded longitudinal space-charge amplifier (LSCA) have been proposed as a mechanism to generate density modulation over a board spectral range. The scheme was recently demonstrated in the optical regime and confirmed the production of broadband optical radiation. In this paper we investigate, via numerical simulations, the performances of a cascaded LSCA beamline at the Fermilab Accelerator Science & Technology (FAST) facility to produce broadband ultraviolet radiation. Our studies are carried using a three-dimensional space charge algorithm coupled with ELEGANT and including a tree-based grid-less space-charge algorithm.

INTRODUCTION

It has been long recognized that collective effects such as coherent synchrotron radiation, wakefield and longitudinal space charge can lead to a microbunching instabilities when combined with bunch compressors (BC) commonly employed in electron linacs. Over the recent years, longitudinal space charge (LSC) has gained considerable interest as a simple mechanism to form attosecond structures on the bunch current distribution for the subsequent generation of intense broadband radiation pulses [1, 2].

The corresponding beamline configuration is relatively simple: it consists of focusing sections (e.g. FODO cells) which ensure the beam size is kept small and where energy modulations due to the space charge impedance accumulate, interspaced with BC sections. The BCs convert the incoming energy modulation into a density modulation. Several of these (FODO+BC) modules are cascaded so to result in a large final density modulation.

Motivated by the recent experimental demonstration of LSCA in the optical regime [2] along with the possible use of high-peak current beams produced in laser-plasma wakefield accelerators [3], we investigate the possible combination of a cascaded LSCA scheme to produce broadband ultraviolet radiation at the Fermilab Accelerator Science & Technology (FAST) facility which couples a high- brightness photoinjector with a superconducting accelerator [4].

* This work was supported by the US Department of Energy under contract DE-SC0011831 with Northern Illinois University. Fermilab is operated by Fermi Research Alliance, LLC under Contract No. DE-AC02-07CH11359 with the US DOE.

SIMULATION METHODS & SETUP

The simulation method employed for our numerical studies has been described elsewhere [5, 6]. In brief we simulate the beam dynamics simulation, including space charge effect, is modeled with the Barnes-Hut algorithm [7] within ELEGANT [8]. The space-charge kicks are applied at discrete user-defined locations using the ELEGANT's `script` command. In its current implementation, the calculations are rather slow (due to files being written out and read in at each space-charge kick location) but the algorithm is being implemented within the ELEGANT main distribution and will eventually be part of future ELEGANT releases.

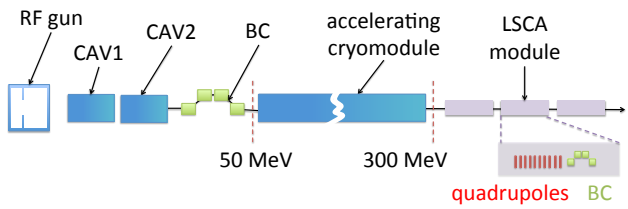

Figure 1: Overview of FAST Facility and the Proposed LSCA. The legend is as follows: "CAVx": accelerating cavities, "BC": magnetic chicane bunch compressor, the red and green rectangles are respectively quadrupole and dipole magnets.

The simulation setup is based on the configuration available at the FAST facility (formerly known as ASTA) [4]; see Fig. 1. In short, the beam is produced from a photocathode located in a $1+\frac{1}{2}$ radiofrequency (RF) gun and accelerated to $\sim$ 50 MeV by two superconducting TESLA cavities. Downstream of the cavities the beam can be manipulated (e.g. longitudinally compressed) and diagnosed before its injection in a ILC-type accelerating cryomodule composed of eight TESLA cavities. Downstream of the cryomodule, the beam, with energy up to $\sim$ 300 MeV, can be injected into the IOTA ring or transported to experiments arranged along a $\sim$ 70 m transport line. Conversely the 70-m beamline, with proper optics, could support the investigation of cascaded LSCAs to produce broadband ultraviolet radiation as discussed in this paper; see also Fig. 1.

Numerical optimization of the electron-beam formation and acceleration to $\sim$ 50 MeV was carried out with ASTRA [9] for various charges. The results combined with a mild bunch compression in the 50-MeV bunch compressor chicane, could produce bunches with peak current of

ISBN 978-3-95450-134-2

$\sim$ 500 A and slice parameters gathered in Table 1 [10]. For simplicity we take all the LSCA modules to be identical: they consist of 4 FODO-cell sections each followed by small-bending-angle chicanes. The introduced dispersion is minimal and does not affect the periodicity of the FODO.

Table 1: Beam Parameters Considered for the LSCA Simulations

Parameter	Value	Units
Lorentz factor, γ	600	–
slice charge, Q	20.0	pC
slice duration, τ	120	fs
peak current I	500	A
slice norm. emittance, $\varepsilon_{x,y}$	5×10^{-8}	m
slice momentum spread, σ_δ	10^{-4}	–
number of macroparticles, N	$[1-10] \times 10^6$	–

The slice was taken to have a Gaussian distributions in the transverse and longitudinal directions. The initial longitudinal phase space was taken to be uncorrelated and the initial Courant-Snyder parameters were matched to the FODO channel.

RESULTS

Optimization of First-stage LSCA

We start with the optimization of one module consisting of several FODO sections and one BC. We varied two parameters at this point - the length of the FODO sections and the bending angle in the chicane which affects its longitudinal dispersion R_{56}. As he goal of this study is to reach the shortest wavelength possible at FAST, we selected the range of very small chicane R_{56} where bunching factor with significant values at high frequency could be attained; see Fig. 2.

The estimated gain per one chicane in LSCA is proportional to the LSC impedance $Z(k,r)$ [3] following $G = Ck|R_{56}|\frac{I}{\gamma I_A}\frac{4\pi L_d|Z(k,r)|}{Z_0}e^{-\frac{1}{2}C^2k^2R_{56}^2\sigma_\delta^2}$, where R_{56} is the BC longitudinal dispersion, $I_A = 17$ kA is the Alfvèn current, L_d is the drift length, σ_δ is the rms fractional energy spread, $C \equiv \langle z\delta\rangle/\sigma_z$ is the chirp, and $Z_0 \equiv 120\pi$ is the free-space impedance. The exponential term in the equation induces a high-frequency cut-off of the modulation $R_{56} \approx -c/(\omega\sigma_\delta)$.

Throughout this paper the bunching factor is computed from the N-macro-particle distribution as $b(\omega) = |\sum_{m=1}^{N} e^{-i\omega t_m}|$ where t_m is the temporal coordinate of the m^{th} macro-particle within the bunch (here $\omega \equiv 2\pi f$ where f is the frequency of observation). We point out that our simulations are performed with $N = 10 \times 10^6$ (while the slice actually contains $N_e = 120 \times 10^6$ electrons). Therefore the noise floor [11] of the bunching factor is $\simeq 1/\sqrt{N_e} \simeq 9 \times 10^{-5}$ while our simulations are limited to noise floor of $\simeq 1/\sqrt{N} \simeq 3 \times 10^{-4}$. Nevertheless we have verified that the gain factor does not depends on the number of macro-particles used in the simulations [12].

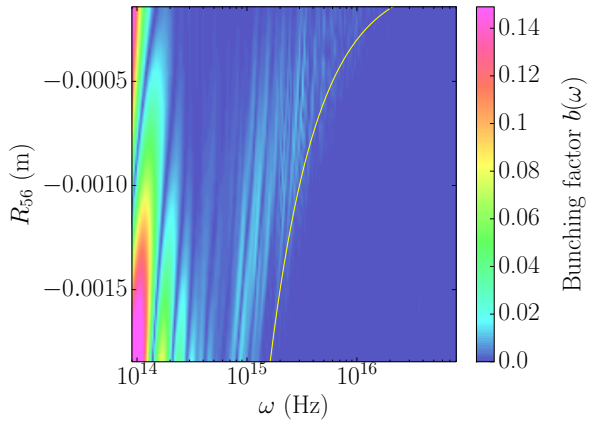

Figure 2: Bunching factor as a function of the longitudinal dispersion R_{56} and observation frequency ω. The yellow line $R_{56} \approx -c/(\omega\sigma_\delta)$ indicates the limit where the microbunching is suppressed due to momentum spread.

The resulting density modulation spectrum is wide and it narrows with the increase of chicane's bending angle. Although the optimal wavelength in this study is around $\lambda_{opt} \approx 650$ nm, the broadband feature of the amplification mechanism actually results in bunching factor enhancement at wavelengths reach the ultraviolet region of the spectrum as illustrated in Fig. 3. The latter figure reports the gain computed as the ratio between the final and initial bunching factors $|b_f(\omega)/b_i(\omega)|$. To smooth out the short-to-shot nature of the gain, the presented gain is average over 20 random realizations of the initial macro-particle distribution.

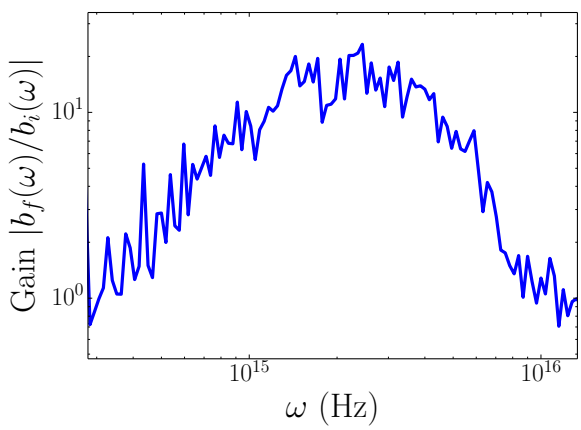

Figure 3: Gain curve as a function of frequency in the interval where significant gain is obtained. The curve is computed for a single (the first) LSCA module.

Simulation of a 3-stage LCSA

To simulate a 3-stage LCSA module, we iterated the process described in the previous section for each stage so to ensure the R_{56} is properly optimized. The simulations were

ISBN 978-3-95450-134-2

carried out in a piecewise fashion: the FODO channel of stage n was simulated with space charge, the output were passed to the subsequent BC. The R_{56} was optimized to provided the largest bunching factor. The optimized values for the R_{56} for first, second and third stage were respectively -3.64×10^{-4}, -2.79×10^{-4}, and -1.42×10^{-4} m.

The resulting distribution was rematched and passed to the $n + 1$ FODO channel where the process was repeated. As aforementioned the chicane have small R_{56} and single-particle dynamics do not affect the matching. However, in the presence of space charge and for a 300-MeV beam, we find that the matching is significantly deteriorated therefore requiring rematching of the beam parameters after each module.

The final phase space and resulting density modulation are presented on Fig. 4. One limitation found in the present study is the cumulated energy spread which leads to transverse emittance growth via chromatic aberration. This emittance dilution eventually leads suppression of the modulation (via an angular smearing effect). Note that at each stage the beam will acquire additional momentum spread which leads to additional emittance Overall this effect result in saturation of the gain in the final stages. For our three stage LSCA we obtained a gain (a the optimum wavelength) $G \approx 500$ for the given beam parameters. The final bunching factor downstream of the third stage appears in Fig. 5 (blue line).

Compressed Case

In addition introducing a longitudinal-phase-space chirp can significantly shift the wavelength region with significant gain to lower wavelength. Thus operating the cryomodule off-crest can compress the modulation wavelength to the ultraviolet regime at FAST: in our studies introducing a chirp $C \equiv \frac{d\delta}{dz}|_0 = 1667\ \mathrm{m}^{-1}$ results in a significant bunching factor (approximately 1%) at $\lambda \approx 140$ nm; see Fig. 5 (green trace). Here we note that for simplicity the chirp was "numerically applied" just before the last bunch compressor (thus its large value). In practice the chirp would be applied before the first LSCA module and therefore would be much smaller.

RADIATION PRODUCTION

Several radiation-production mechanisms can be considered. For simplicity we consider the case of a planar undulator. Given the beam energy of 300 MeV, and taking a undulator parameter of $K = 0.1$ yields a resonant wavelength $\lambda \simeq 1.4 \times 10^{-6} \lambda_u$, for an undulator period λ_u (corresponding to $\omega = 1.35 \times 10^{15}/\lambda_u$). A 10-cm undulator period will results in a frequency $\omega \simeq 1.2 \times 10^{16}$ s^{-1} where the bunching factor scaled for 120M macroparticle is $5 \sim 10^{-2}$; see Fig. 5 (red trace). Simulations performed with GENESIS [13] (in steady state mode) indicate that a radiation energy of $\mathcal{E} \simeq 3$ ţJ could be reached.

SUMMARY

Using a grid-less code adapted from Astrophysics we have investigated the effect of three-dimensional LSC impedance

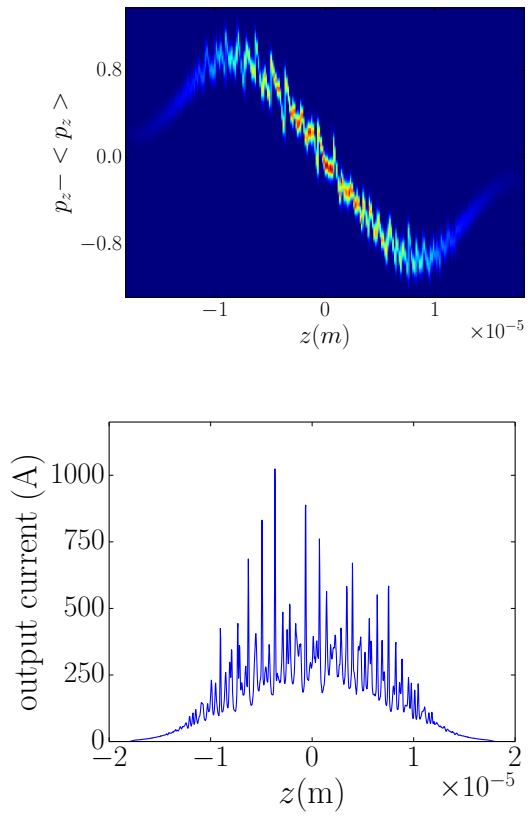

Figure 4: Longitudinal phase space (top density plot) and resulting density modulation (bottom plot) downstream of the third LSCA stage for $N = 10 \times 10^6$ macro-particles.

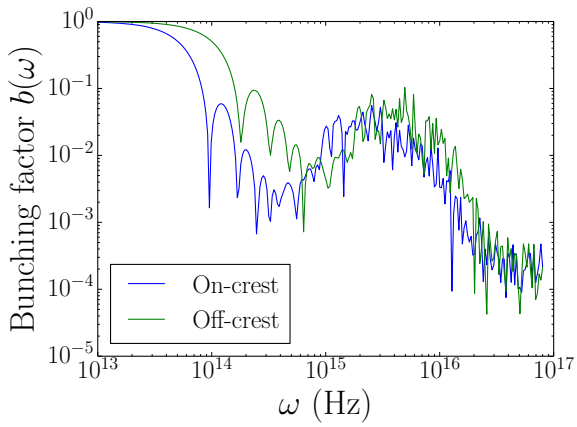

Figure 5: Simulated bunching factor downstream of the third LSCA stage for the case of an uncompressed (blue) and compressed (green) incoming beam.

and found that the possible use of a cascaded LSCA scheme at FAST can produce femtosecond microstructures in the longitudinal phase space with a period ranging from 140 to 700 nm. Our study involves beam parameters comparable to the ones achievable at FAST.

ISBN 978-3-95450-134-2

REFERENCES

[1] E. A. Schneidmiller and M. V. Yurkov, Phys. Rev. ST Accel. Beams **13**, 110701 (2010).

[2] A. Marinelli, E. Hemsing, M. Dunning, D. Xiang, S. Weathersby, F. O'Shea, I. Gadjev, C. Hast, J. B. Rosenzweig, Phys. Rev. Lett. **110** 064804 (2013).

[3] M. Dohlus, E. Schneidmiller, M. V. Yurkov, C. Henning, F. J. Grüner, Proc. SPIE **8779**, 87791T (2013).

[4] E. Harms, J. Leibfritz, S. Nagaitsev, P. Piot, J. Ruan, V. Shiltsev, G. Stancari, A. Valishev, ICFA Beam Dyn.Newslett. **64** 133 (2014).

[5] A. Halavanau, P. Piot, in Proc. of the 2015 International Accelerator Conference (IPAC15), Richmond, VA, USA, 1853 (2015)

[6] A. Halavanau, P. Piot, ibid [5], p. 1850 (2015).

[7] J. Barnes and P. Hut, Nature, **324**, 446 (1986).

[8] M. Borland, Advanced Photon Source, Note LS-287, available from Argonne (unpublished 2000).

[9] P. Piot, Y.-E Sun, M. Church, in Proc. of the 2010 International Accelerator Conference (IPAC10), Kyoto, Japan, 4316 (2010).

[10] C. R. Prokop, P. Piot, B. E. Carlsten, M. Church, Nucl. Instrum. Meth. Sec. A **716**, 17 (2013).

[11] C. J. Hirschmugl, M. Sagurton, G. P. Williams, Phys. Rev. A **44**, 1316-1320 (1991).

[12] A. Halavanau, P. Piot, manuscript in preparation (2015).

[13] S. Reiche, Nucl. Instrum. Meth. Sec. A **429**, 243 (1999).

ISBN 978-3-95450-134-2